AN INHALATION DOSE MODEL FOR ASSESSING DUST–BORNE VOC–ODOR EXPOSURE FROM FEEDING IN SWINE BUILDINGS

C. M. Liao, J. W. Chen, M. Y. Huang, J. S. Chen, T. J. Chang

ABSTRACT. *A dynamic, size–dependent integrated inhalation dose model for quantifying worker/animal exposure to dust–borne odor causing volatile organic compounds (VOC–odor) in swine buildings during and after feeding was developed. The exposure of dust–borne VOC–odor observed in pig barns can be characterized by adsorption and deposition of airborne dust. The airborne dust particle size, aerosol profile, enclosure dimension, ventilation rate, and feeding duration were affecting the integrated inhalation model in assessing dust–borne VOC–odor exposure during and after the time of feeding. Experimental results show that there is no significant variation in feeding and non–feeding periods for the particle size distributions in a growing pig farm located in southern region of Taiwan and both followed a lognormal distribution with geometric mean diameter of 2.14 ±0.03 μm (mean ±1 sd) and geometric standard deviation of 1.73 ±0.02. Mean total dust mass concentrations were 20.47 ±8.23 and 2.32 ±0.45 mg m^{-3}, respectively, for feeding and non–feeding periods. Model simulations show that the inhalation dose for a short feeding duration followed by a long stay in the pig barn can equal that of a long feeding duration followed by a short subsequent exposure. Reduction of both the feeding duration and/or subsequent time in the pig barn is highly effective in dose reduction.*

Keywords. *Dust, Adsorption, Deposition, Exposure, Odor, VOC.*

Dust is one of the main air contaminants in swine buildings and results from animal activity, air movement, finely ground dry feed introduced during feeding, and fecal–feed particles deposited on a solid floor and later entrained into the air. During pig non–feeding periods, dust particles tend to settle out, whereas they can be continuously reintroduced into the airspace during feeding periods. Zhang et al. (1996) and Perkins and Feddes (1996) indicated that the majority of particles are of fecal origin, however, the major proportion (85%) of the dust mass in swine buildings is from feed particles. Perkins and Feddes (1996) further pointed out that feed dust is not the major problem; it's the result of animal movement during that time.

Odor–causing volatile organic compounds (referred to as VOC–odor) from manure are a complex mix of chemicals. Hammond et al. (1974), Yasuhara and Fuwa (1979a, 1979b, 1979c), Yasuhara (1980), and Yasuhara et al. (1983, 1984) have identified more than 150 VOC–odors in solid manure, liquid manure, and gases emitted from manure and dust in swine buildings. Hammond et al. (1979) identified 10 VOCs in the air from swine buildings that were the source of suspended particulate matter concentrations of VOC–odor. Miner (1982) and Barth et al. (1982) pointed out that VOC–odors exhausted from farm buildings were often associated with airborne dust particles. Hangartner (1990) indicated that filtering dust from the exhaust air reduced VOC–odor emissions from swine buildings by up to 65%. The collective evidence suggests a high correlation between VOC–odor and existing aerosol in swine buildings.

The source–term for VOC–odor is inherently time–dependent. VOC–odor enters the ventilated airspace from manure pit, and a substantial fraction of it is adsorbed to the existing aerosol to yield a size–distributed, particle–phase VOC–odor. The principal factors governing the levels of dust–borne VOC–odor include animal activity, floor dryness contribute to dust emission rates, the adsorption of VOC–odor to an airborne particle, the deposition on enclosure surfaces, and removal by air exchange. Little information currently exists on the size distribution and behavior of dust–borne VOC–odor during the time of feeding.

Phenomena such as turbulent coagulation, diffusiophoresis, and thermophoresis can also influence the dust–borne VOC–odor concentration (Liao and Feddes, 1991; 1992). The contributions from these effects, however, are typically small (Liao and Feddes, 1991; 1992) and are neglected in this model. Generally, turbulent coagulation becomes very important for particles larger than 10 μm aerodynamic equivalent diameter (AED) (Hinds, 1999) and the majority of dust particles found in animal housing have diameter that ranged between 0.5 and 5 μm AED (Gao and Feddes, 1993; Van Wicklen and Yoder, 1988).

The concentration gradients are not expected to be large enough to make diffusiophoresis significant. Since air circulation is modeled isothermally, temperature gradients will not be established in the ventilation flow field.

Article was submitted for review in July 2000; approved for publication by the Structures & Environment Division of ASAE in July 2001.

The authors are **Chung–Min Liao**, ***ASAE Member***, Professor, **Jein–Wen Chen**, Graduate Research Assistant, **Mei–Yu Huang,** Graduate Research Assistant, and **Tsang–Jung Chang**, ***ASAE Member Engineer***, Assistant Professor, Department of Bioenvironmental Systems Engineering, National Taiwan University, Taipei, Taiwan; and **Jui–Sheng Chen**, Assistant Professor, Department of Environmental Engineering and Sanitation, Foo–Yin Institute of Technology, Kaohsing, Taiwan. **Corresponding author:** Chung–Min Liao, Dept. of Bioenvironmental Systems Engineering, National Taiwan University, Taipei, Taiwan 10617 Republic of China, phone: +886–2–23634512, fax: +886–2–23626433, e–mail: cmliao@ccms.ntu.edu.tw.

  ISSN 0001–2351

Additionally, there could be hygroscopic growth in the high humidity environment of the animal housing. Hygroscopic growth is so rapid (Hinds, 1999) that it can be considered as a transient that occurs before VOC–odor adsorbs to the existing aerosol.

In this article, well–defined physical models are used to develop the dynamic model for the underlying physical phenomena. Adsorption of VOC–odor to the existing aerosol is relatively well understood and could be refined from an adsorption model based on the homogeneous surface diffusion theory (Liao and Singh, 1998).

Deposition is more complex. Even though diffusiophoresis and thermophoresis can be neglected, Brownian and turbulent diffusion, sedimentation, and laminar as well as convective flow exist to varying degrees and lead to particle deposition onto walls and other surfaces. Depending on the flow regime, different models have been proposed for particle deposition in a ventilated airspace. The turbulent flow scheme appears to be best applicable to a ventilated airspace in which turbulent flow is a typical feature of the airflow. In the present work we adopted a mathematical model derived by Crump and Seinfeld (1981) for the rate of aerosol deposition in a turbulence mixing enclosure of arbitrary shape under the assumption of homogeneous turbulent near the surfaces. Crump and Seinfied's deposition model, which is a refinement of Corner and Pendelebury's analysis (Corner and Pendelebury, 1951), forms the basis of deposition studies and was adopted in the present research.

The goal of this work is to incorporate the time– and size–dependent dust–borne VOC–odor concentration from the dynamic model with the size–dependent inhalation dose factor to obtain the integrated exposure dose model as a function of size and time. In this article we evaluate the worker/pig exposure to dust–borne VOC–odor during and after feeding in terms of observed particle size distributions and dust levels. Our present purpose is not to model dust–borne VOC–odor transport in swine buildings, but rather to semi–quantitatively explore the role of adsorption and deposition in controlling the exposure of dust–borne VOC–odor observed in pig barns.

MODEL FORUMULATION

DYNAMIC MODEL

Combining the physical processes controlling the gain and loss rates, the decay of VOC–odor, the adsorption of VOC–odor to airborne dust, the deposition (including Brownian and turbulent diffusive deposition and gravitational sedimentation), and air exchange, yields the dynamic equations that describe the concentration trajectory of VOC–odor and dust–borne VOC–odor in a ventilated airspace.

Followed by the principle of mass balance, the dynamic equations varying with particle size range k and time t are given by:

$$\frac{dC_V(t)}{dt} = V^{-1}S(t) - \left(\lambda_i + \lambda_v + \sum_{k=1}^{N-1}\lambda_a(k)\right)C_V(t) \qquad (1)$$

$$\frac{dC(k,t)}{dt} = \lambda_a(k)C_V(t) - [\lambda_v + \lambda_d(k)]C(k,t), k = 1, 2, \ldots, N-1 \qquad (2)$$

where

$C_v(t)$ = time–dependent VOC–odor concentration (kg m^{-3})
$S(t)$ = VOC–odor source strength (kg h^{-1})
V = air volume (m^3)
λ_i = first–order decay rate constant of VOC–odor (h^{-1})
λ_v = air exchange rate (h^{-1}) in which $\lambda_v = Q/V$
Q = ventilation rate (m^3 h^{-1})
$C(k,t)$ = time–dependent dust–borne VOC–odor concentration in the kth size range (kg m^{-3})
$\lambda_a(k)$ = rate of adsorption of VOC–odor to aerosol surface in the kth size range (h^{-1})
$\lambda_d(k)$ = deposition rate of dust–borne VOC–odor due to Brownian and turbulent diffusive deposition and gravitational sedimentation in the kth size range (h^{-1})
k = size range number
N = assigned to be the end point number for a kth size range, d_k and d_{k+1} .

Specifically, the left–hand side of equation 2 describes the rate at which the concentration of dust–borne VOC–odor of size range k changes with time. The first term on the right–hand side of equation 2 expresses the formation rate of dust–borne VOC–odor of size range k from VOC–odor by adsorption. The second term describes the loss of dust–borne VOC–odor of size range k by air exchange and deposition.

The particles are divided into geometrically equal sized bins in the size range of interest. The dust–borne VOC–odor or airborne dust concentration is assumed to be a constant diameter within each bin size. The end points, d_k and d_{k+1} , of the kth bin size are considered to be equal to the logarithmic mean of the end points of the bin size as,

$$\ln d_k = \ln d_{min} + \frac{(\ln d_{max} - \ln d_{min})(k-1)}{N-1}, k = 1, 2, \ldots, N \qquad (3)$$

where particles smaller than d_{min} (the minimum diameter) are considered to be the finest, and d_{max} is the largest particle size of interest.

MODEL LIMITATIONS

In the development of the model the following assumptions are made to simplify some physiochemical aspects: (1) the ventilation airflow system is assumed to be a complete mixing system, (2) every particle is treated as an aerodynamic equivalent sphere and is electrically neutral, (3) no gas–to–particle conversion occurs within the system, (4) mass transfer resistance from bulk VOC–odor to outer surface of dust particles and turbulent coagulation of dust– and adsorbed–phase are negligible, (5) bulk VOC–odor concentration is in equilibrium with the adsorbed phase concentration at the particle surface, and (6) VOC–odor is assumed to be adsorbed on the outer surface first, then enter the dust particle through surface diffusion, and eventually occupy adsorption sites in the inner surface.

We acknowledge that some assumptions we made violated actual conditions. The development and application of the dynamic approach in our proposed form does not derive from an *a priori* assumption that building airflow systems are inherently "well–mixed" but from the practical view that seeks to extract the maximum usefulness from the "well–mixed" approach before accepting the complexities attending "heterogeneous mixed" approaches. Several real

advantages of the "well–mixed" approach include: (1) computational simplicity, (2) ease of calibration for well–characterized systems, and (3) capacity of extrapolating to other uncharacterized systems. Philosophically, it can be argued that parsimony is a legitimate modeling objective and additional model complexity (often in the form of nonlinearity) should only be advocated if it can be shown to significantly reduce uncertainties normally attributed to random system or measurement errors. In the case of our present work, it is hoped that additional experimental data with well–documented test information can be used to confirm or reject the overall applicability of a comparable approach that we employed to modeling indoor air quality problems.

Parametrization of Rate Equations

Solution of equations 1 and 2 requires that the adsorption rate and deposition rate over the various *k*th size ranges be estimated. Parametric forms for the adsorption and deposition rates used in interaction algorithm of dynamic model are given in table 1. The role of each rate equation will be investigated.

Adsorption Rate

Based on the formulas derived by Liao and Singh (1998) (referred to as the L–S model), the adsorption coefficient ($m^3\,h^{-1}$) can be obtained from homogeneous surface diffusion theory. The Freundlich isotherm is widely used to describe sorption equilibrium in environmental systems with heterogeneous surfaces (Weber and DiGiano, 1996). Although in this article airborne dust is superficially assumed to be homogeneous, significant heterogeneity likely exists. Additionally, over time, airborne dust surfaces slowly react by means of physicochemical or biological processes, which may have further contribute to surface heterogeneity. The L–S model, however, is purely theoretical and absent empirical verification, must be applied with caution. Adsorption rate equations that appear in equations 4–6 imply that: (a) airborne dust particles in animal housing are usually not homogeneous in size and (b) the lognormal probability density function (pdf) is the most common used distribution for characterizing aerosol particle size.

Deposition Rate

The deposition rate model used in this work is adopted from Crump and Seinfeld (1981) and is referred to as the C–S model. The C–S deposition model is a refinement of Corner and Pendelebury's analysis (Corner and Pendelebury, 1951). Depending on the flow regime, different models have been proposed for particle deposition in a room. The turbulent flow paradigm appears to be best applicable to the feeding scenario where ventilation (natural or forced) is the primary source of turbulent. The C–S model is a well–established general model for the rate of aerosol deposition due to turbulent diffusion, Brownian diffusion, and gravitational sedimentation in a turbulently mixed, enclosed enclosure of arbitrary shape. Application of the C–S model to a rectangular enclosure yields equation 10 for the deposition rate of a specific particle diameter, d_p. The deposition rate for the *k*th size bin of equation 9 is obtained by integrating equation 10 over the whole bin. The C–S model was developed for reactor vessels where turbulence is produced by stirring. The turbulence parameter (k_e) was estimated by assuming complete turbulent dissipation of the input energy. It is difficult to estimate k_e when turbulence is induced by ventilation. In the present analysis, the estimates of k_e were

Table 1. Rate equations for adsorption and deposition used in the dynamic model. (The description of symbols is given in the Appendix.)

Adsorption rate: $\lambda_a(k)$ **Eq.**

$$\lambda_a(k) = Z\int_{d_k}^{d_{k+1}} \beta(d_p) f(d_p)\, d(d_p) \quad (4)$$

where

$$\beta(d_p) = K_F C_{v,e}^{n_F - 1}\left(\frac{3}{\Phi^2(d_p)}\left(\Phi(d_p)\coth(\Phi(d_p)) - 1\right)\right) Q\sigma_p \quad (5)^{[a]}$$

$$f(d_p) \equiv LN(d_g, \sigma_g) = \frac{1}{\sqrt{2\pi}\, d_p \ln\sigma_g}\exp\left(-\frac{(\ln d_p - \ln d_g)^2}{2(\ln\sigma_g)^2}\right) \quad (6)^{[b]}$$

$$\Phi(d_p) = \frac{d_p}{\sqrt{D_s\bar{\tau}}} \quad (7)^{[c]}$$

$$\bar{\tau} = \frac{V}{Q} \quad (8)$$

Deposition rate: $\lambda_d(k)$

$$\lambda_d(k) = \frac{1}{d_{k+1} - d_k}\int_{d_k}^{d_{k+1}} \lambda_d(d_p)\, d(d_p) \quad (9)$$

where

$$\lambda_d(d_p) = \frac{1}{lwh}\left\{(2wh + 2hl)\left(\left(\sin\frac{\pi}{n}\right)(k_e D(d_p)^{n-1})^{1/n}\right) + wlv_s(d_p)\coth\left(\frac{\pi v_s(d_p)}{2\left(n\sin\frac{\pi}{n}\right)(k_e D(d_p)^{n-1})^{1/n}}\right)\right\} \quad (10)^{[d]}$$

$$D(d_p) = \frac{k_B T C_{slip}}{3\pi\eta_a d_p} \quad (11)^{[b]}$$

$$v_s(d_p) = \frac{\rho_p g d_p^2}{18\eta_a} C_{slip}\left[1 - \frac{\rho_a}{\rho_p}\right] \quad (12)^{[b]}$$

$$C_{slip} = \left(1 + \frac{\lambda}{d_p}\left(2.541 + 0.8\exp\left(-0.55\frac{d_p}{\lambda}\right)\right)\right) \quad (13)^{[b]}$$

[a] Derived based on Liao and Singh (1998).
[b] Adopted from Hinds (1999).
[c] Adopted from Liao and Singh (1998)
[d] Adopted from Crump and Seinfeld (1981).

obtained from indoor air based on airflow velocities in the room by Nazaroff and Cass (1989) and Nazaroff et al. (1990).

Source Strength of VOC–Odor

The scenario of the stored manure pit can be described as follows: (1) the contaminated source is uniformly distributed in the thickness of the contamination layer, (2) VOC–odor may reside in three phases in the contaminated layer zone: an adsorbed phase, a dissolved phase, and a gaseous phase, (3) the adsorbed and dissolved phases are assumed to undergo reversible and linear equilibrium adsorption, while dissolved and gaseous phases are assumed to be in equilibrium in accordance with the Henry's law, (4) the swine manure properties such as total porosity, gas–filled porosity, bulk density, fraction of organic carbon, pH, and temperature are assumed to be constant in space and time, (5) the VOC–odor moves in one dimension through the swine manure, (6) VOC–odor enters into the ventilated airspace by advection where a complete mixing airflow system is assumed, and (7) swine manure is assumed to be isotropic and homogeneous.

Jury et al. (1990) estimated the effect of steady–state moisture movement (advection) on chemical volatilization rates from contaminated soil. When manure moisture movement is involved, the VOC–odor flux from the stored swine manure, $J_s(0,t;W)$, can be expressed based on the behavior assessment model of Jury et al. (1990) as:

$$J_S(0,t;W)=\frac{1}{2}C_S\exp(-\lambda_i t)\left\{V_E\left[erfc\left(\frac{V_E t}{\sqrt{4D_E t}}\right)\right.\right.$$

$$\left.-erfc\left(\frac{W+V_E t}{\sqrt{4D_E t}}\right)\right]+(2H_E+V_E)\times\exp[H_E(H_E+V_E)t/D_E]$$

$$\left[\exp(H_E W/D_E)\times erfc\left(\frac{W+(2H_E+V_E)t}{\sqrt{4D_E t}}\right)\right.$$

$$\left.\left.-erfc\left(\frac{(2H_E+V_E)t}{\sqrt{4D_E t}}\right)\right]\right\} \qquad (14)$$

where

$J_s(0,t;W)$ = time–dependent VOC–odor flux from manure pit (g m^{-2} s^{-1})
C_s = initial VOC–odor concentration in slurry column (g m^{-3})
W = contaminated layer thickness of slurry (m)
D_E = effective diffusion coefficient of VOC–odor in the slurry (m^2 s^{-1})
H_E = horizontal moisture velocity (m s^{-1})
V_E = vertical moisture velocity (m s^{-1}).

The time–dependent VOC–odor source strength therefore has the following form:

$$S(t)=J_S(0,t;W)A \qquad (15)$$

where A is the manure pit area (m^2). Equation 14 has been used to evaluate indoor inhalation exposure dynamics of VOC–odor volatilization from stored pig slurry (Liao and Liang, 2000). The key parameter in equation 14 is the effective diffusion coefficient (D_E) and vertical moisture velocity (V_E). According to the model developed by Jury et al. (1990), the effective diffusion coefficient defines the rate of mass transfer between the liquid and gas phases. Thus D_E depends on the combined mass transfer through liquid and gas boundary layers. Equation 14 also shows that VOC–odor concentration is affected by constant moisture contents and steady–state moisture advection.

The diffusive component is described by a manure diffusion coefficient that is a function of the Henry's law constant, the diffusion coefficient of VOC–odor in both air and water, the adsorption coefficient of the VOC–odor to the manure, manure water content, porosity, and manure bulk density. Partitioning of VOC–odor between the vapor, aqueous, and sorbed phases is assumed to be at equilibrium at all times. The advection component is controlled by a user–specific manure moisture flux rate that is held constant as a function of time.

Inhalation Dose Model

The time–dependent concentration profiles of dust–borne VOC–odor are used to calculate cumulative exposure doses through inhalation. The cumulative dose is calculated from the formula:

$$D(k,t)=\frac{\gamma(k)}{B_w}\int_0^t C(k,t)B_r(t)dt \qquad (16)$$

where

$D(k,t)$ = time–dependent cumulative exposure dose of dust–borne VOC–odor per unit body weight of worker or animal in the kth size bin (μg kg^{-1})
$\gamma(k)$ = fraction of the dust–borne VOC–odor taken into the total lung volume that is available for uptake for the kth size bin
B_w = body weight of the worker or animal (kg)
$B_r(t)$ = breathing rate of the worker or animal at time t (L min^{-1}).

In this study, we assume all of the dust–borne VOC–odor for each size bin taken into the lung is available for uptake, i.e., $\gamma(k)=\gamma=1$.

The differences in exposure can vary due to factors such as pen dimensions, ventilation rate, and aerosol profile in the room. Additionally, differences in feeding strategies including duration of the feeding and the number of consecutive feedings also influence the exposure. The time–dependent size distribution of dust–borne VOC–odor from the dynamic model of equations 1 and 2 was combined with cumulative dose model (16) for the size–dependent dose to obtain the integrated inhalation dose as a function of size.

Numerical Schemes

The system of equations 1 and 2 is a linear, first–order system of coupled differential equations. Integration over time is straightforward in principle but is complicated by the existence of a large number of widely differing time scales. The number of independent variables is $2N+1$ where N is the number of bins in the size range of interest. The numerical integration scheme used to solve the system dynamic equations 1 and 2 is a subroutine (DIVPRK) based on the Runge–Kutta–Verner 5th–order and 6th–order method, whereas a subroutine (QDAG) based on Gauss–Legendre

formulas is adopted to solve equation 16. Both subroutines are provided by IMSL Subroutines Library (IMSL MATH/ LIBRARY, 1994) and are processed in double precision with FORTRAN 90. The algorithm is stable provided the error and the convergence criterion are carefully monitored.

EXPERIMENTS

An experiment was carried out to characterize the particle size distributions and dust levels for the existing airborne dust during feeding and non–feeding periods.

A growing pig farm located at Tainan, a southern region of Taiwan, was chosen as our study area. Measurements were conducted in a fan–ventilated swine building (fig. 1). The building with a semi–slatted floor had dimension of 24 m × 9.2 m × 2.0 m. There were two manure pits measuring 1 m × 23 m along each side of room. Six 4.0 m × 4.0 m pens on each side of the room were separated by a 1.2 m wide service alley. One 0.9 m diameter fans located at the end of the building with continuous slot eave inlets provides summer ventilation. During the experiment, fan was operated continuously. Building ventilation rates, determined using the impeller method developed by Liu (1997) and the manufacturer specification, were 845 ±15 and 280 ±11 m^3 h^{-1}, respectively, during feeding and non–feeding periods. There were 150 pigs in the room at a stocking density of 10–15 pigs/ pen. Indoor air temperature and relative humidity were 29°C ±1.5°C and 54% ±3%, respectively.

The type of feed used in the Tainan swine building is made from the very fine feedstuff powder and without any oil or liquid matter mixed with. The feed powder looks like the milk powder, fine and easy to become airborne. The amount of feed consumed in each feeding period is about 2 kg/pig. The feeding method is the mechanical drop associated with the manual. In order to know the particle size distribution of the feed used in the Tainan swine building, we have also conducted a chamber test to determine the particle size distribution of the feed.

A portable laser dust monitor (Series 1100, Grimm Labortechnik GmbH & Co. KG, Ainring, Germany; referred to as DM1100) was used to analyze the airborne dust characteristics. The DM1100 combines the principles of aerodynamic particle size separation and light scattering particle detection. The AED of the particles can range from 0.5 to 10 μm. The DM1100 measured dust mass concentrations in the range of 1.0 to 50000 μg m^{-3}. Measured channels are in the ranges of 0.5–1, 1–2, 2–5, 5–10, and >10 μm aerodynamic diameter. Before the measurements, the DM1100 was calibrated with known particles of Uniform Latex Microspheres Polystyrene (0.5 μm) and Polymer Microspheres Styrene Vinyltoluene (3 μm) (Duke Scientific, Palo Alto, Cal.). The sampling interval was divided into three periods: 06:00–07:00 (1st feeding period), 07:00–18:00 (non–feeding period), and 18:00–19:00 (2nd feeding period).

Monitoring commenced when the pigs were 150 days old (mean pig weight = 70 kg). Dust sampling was conducted for 5 sampling days. The DM1100 was operated at the design sampling flow rate of 1.2 L min^{-1}±10%. There were three measuring plans (A, B, and C) in that each measuring plan had four measuring locations (fig. 1). Sampling time was 3 min for each sampling location in that DM1100 needs 5 s to record each reading. It took nearly 1 h to measure the

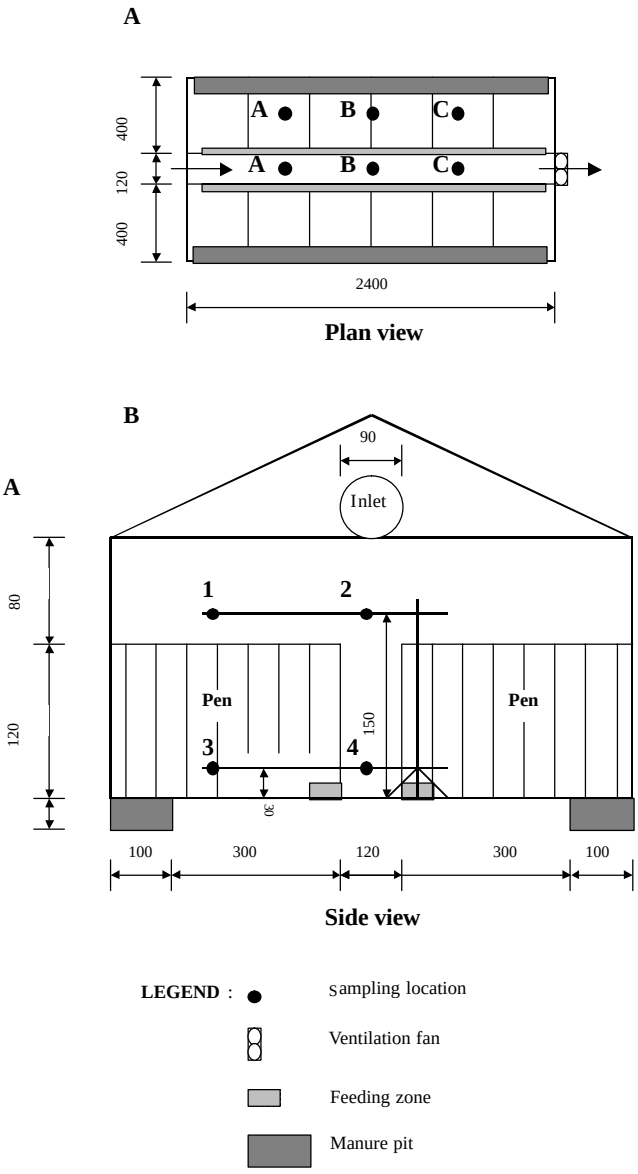

Figure 1. Schematic diagram of the Tainan swine building showing the sampling locations: (A) plan view, and (B) side view. All dimensions are in centimeter (cm).

concentrations at all 12 sampling locations. The outputs from DM1100 can be expressed both as μg m^{-3} and as particles L^{-1}. A portable IBM PC was used to collect all sampling data.

INPUT PARAMETERS

Number of bins and size ranges. In this study, the size range from 0.5 to 5 μm was divided into five geometrically equal size bins based on equation 3. Resulting values of the average particle diameter were 0.95, 1.85, 2.75, 3.65, and 4.55 μm for bins 1, 2, 3, 4, and 5, respectively.

Source strength parameters. In order to obtain the effective diffusion coefficient (D_E) that is expressed as follows (Jury et al., 1990):

$$D_E = \frac{(\varepsilon_a^{10/3} D_g^a K_H + \theta^{10/3} D_l^w)/\varepsilon^2}{(\rho_b f_{oc} K_{oc} + \theta + \varepsilon_a K_H)} \qquad (17)$$

We tried to select the chemical database of VOC–odor that is already in hand. In equation 17, the physiochemical properties of toluene such as Henry's law constant (K_H), and air and water diffusion coefficients (D_g^a, D_l^w), organic carbon distribution coefficient (K_{oc}), and fraction of organic carbon (f_{oc}) are well documented (Howard et al., 1991; Thibodeaux, 1996). Toluene is also the one of intense odor causing VOCs found in swine buildings. Therefore, we chose toluene as our study compound in this present work. The value of effective diffusion coefficient of toluene (D_E) is calculated to be 1.05×10^{-9} m^2 s^{-1} corresponding to moisture content of 80% (Liao and Liang, 2000).

Adsorption rate parameters. Often one finds $0 < n_F \leq 1$ for Freundlich exponents. An $n_F = 1$ is used in present analysis to simplify the model simulation for expedient computation. Van Loy et al.(1997) have shown that the linear model correctly captures the dynamics of VOC sorption on indoor materials. The value of the surface effective air diffusivity of VOC–odor (D_s) in the adsorption rate model was taken from the value of air diffusivities at temperature of 29°C for toluene. The resulting value is 8.8×10^{-6} m^2 s^{-1} (Liao and Liang, 2000). Freundlich capacity constant (K_F) was estimated to be 0.2 m^3 kg^{-1} corresponding to $n_F = 1$ (Geankoplis, 1993).

Deposition rate parameters. In the C–S model, the value of the exponent (n) was chosen to be 2 (Nazaroff et al., 1990). The value of the turbulent intensity parameter, k_e, was set equal to 0.5 s^{-1} to correspond to the indoor air in a room with an operating fan (Nazaroff et al., 1990; Nazaroff and Cass, 1989). There will be some coupling between the rate of ventilation and the degree of turbulence. This coupling is small for ventilation–induced turbulence and was neglected in the model.

Table 2 summarizes the values of all the input parameters appearing in the models. Table2 shows the indoor temperature is held fixed at 29°C. Calculations using the model developed for this work indicate that, ignoring thermophoretic forces, a change in temperature from 20°C to 35°C has a negligible effect on the adsorption and deposition rates. Since the goal of this work was to examine the dynamic contribution to exposure dose from feedings, the initial conditions for the gas–, adsorbed–, and particle–phase concentrations for all the simulations were assumed to be zero. Table 3 summarizes the operating parameters used in the model simulations. The aerosol profile was assumed to be time–independent during each individual simulation.

Table 2. A summary of input parameters appearing in model implementation.

Parameter	Description	Representation values
VOC–odor source strength		
D_E	Effective diffusion coefficient of toluene	1.05×10^{-9} m^2 s^{-1}[a]
V_E	Effective moisture velocity (advection)	8.64×10^{-4} cm d^{-1}[a]
H_E	Effective moisture horizontal velocity	0[a]
W	Thickness of contaminated layers	W = 10 cm
A	Manure pit area	2×23 m^2
λ_i	1st–order decay rate constant of toluene	3.2×10^{-2} d^{-1}[a]
C_s	Assumed initial toluene concentration in slurry	5 mg L^{-3}[a]
Adsorption rate		
D_s	Surface effective diffusivity of toluene in air	8.8×10^{-6} m^2 s^{-1}[a]
K_F, n_F	Parameters of Freundlich isotherm	K_F = 0.2, n_F = 1[b]
$C_{v,e}$	Steady–state VOC–odor concentration	4.12 μg m^{-3}[c]
Deposition rate		
$V = l \times w \times h$	Pig house dimension	l = 24 m, w = 9.2 m, h = 2 m
n	Exponent constant	2[d]
k_e	Turbulent intensity parameter	0.5s^{-1}[e]
η_a	Dynamic viscosity of air	1.85×10^{-4} P[f]
ρ_a	Density of air	1.18×10^{-3} g cm^{-3}[f]
K_B	Boltzmann's constant	1.38×10^{-16} erg °K^{-1}[f]
T	Indoor absolute temperature	302°K
λ	Mean free path of air	0.66×10^{-5} cm[f]
ρ_p	Particle density	1.0g cm^{-3}

[a] Adapted from Liao and Liang (2000).
[b] Adopted from Geankoplis (1993).
[c] Calculated based on Equation 1.
[d] Adopted from Nazaroff et al. (1990).
[e] Adopted from Nazaroff et al. (1990) and Nazaroff and Cass (1989).
[f] Adapted from Hinds (1999).

Table 3. Operating parameters used in the model simulation.

	Feeding period	Non–feeding period
Ventilation rate	845 m^3 h^{-1}	280 m^3 h^{-1}
Aerosol profile		
Particle size distribution	LN(2.17, 1.75)	LN(2.11, 1.71)
Particle concentration	3980 cm^{-3}	455 cm^{-3}
Dust source conc. in each bin (particles cm^{-3})		
Bin 1 (0.5~1.4 μm)	478	54
Bin 2 (1.4~2.3 μm)	1791	204
Bin 3 (2.3~3.2 μm)	796	92
Bin 4 (3.2~4.1 μm)	597	68
Bin 5 (4.1~5.0 μm)	318	37
Breathing rate (L min^{-1})[a]		
Growing pig	20	6.6

[a] Data are adapted and calculated from DeJours (1968) and Mount (1968).

RESULTS AND DISCUSSION

Table 4 gives the experimental results for each measuring period. Experimental results show that the particle size distributions followed a lognormal distribution with geometric mean diameters (GMD) (which is based on number) of 2.17 ±0.06 and 2.11 ±0.05 μm and geometric standard deviation (GSD) of 1.75 ±0.05 and 1.71 ±0.06 during feeding and non–feeding periods, respectively. Figure 2 presents the lognormal size distribution model fitted to the experimental data for feeding and non–feeding periods. Table 4 indicates that the mean total dust mass concentrations were 20.47 ±8.23 mg m^{-3} (ranging from 15.37–29.44 mg m^{-3}) and 2.32 ±0.45 mg m^{-3} (ranging from 1.76–2.80 mg m^{-3}), respectively, for feeding and non–feeding periods. The result from the chamber test shows that the particle size distribution of the feed is LN(2.13, 1.7), indicating that feed dust were the main source of the airborne dust. A comparison with the published data (9.0–18.6 particles cm^{-3}) (Van Wicklen and Yoder, 1988) shows that the magnitude of the number concentrations observed in the Tainan swine building

Table 4. Experiment results of airborne dust concentrations (Mean ±S.D., *n* = 180) and geometric mass mean diameter (GMD) and geometric standard deviation (GSD) for each measuring period carried out in the Tainan growing pig farm

	06:00–07:00 (1st feeding period)			12:00–13:00 (Non–feeding period)			18:00–19:00 (2nd feeding period)		
Sampling Location[a]	Concentration (mg m^{-3})	GMD (μm)	GSD (–)	Concentration (mg m^{-3})	GMD (μm)	GSD (–)	Concentration (mg m^{-3})	GMD (μm)	GSD (–)
A1	12.05 ±4.21	2.11	1.69	2.08 ±0.65	2.01	1.62	11.77 ±2.01	2.07	1.69
A2	20.9 ±6.1	2.20	1.81	1.98 ±0.94	2.08	1.7	25.3 ±7.2	2.22	1.75
A3	16.11 ±4.32	2.16	1.75	2.41 ±0.22	2.16	1.68	16.33 ±4.61	2.16	1.73
A4	27.01 ±9.02	2.06	1.75	2.0 ±1.01	2.09	1.69	23.53 ±8.11	2.26	1.73
B1	17.33 ±2.19	2.11	1.71	2.33 ±0.4	2.08	1.68	18.89 ±2.46	2.23	1.75
B2	31.22 ±6.57	2.21	1.74	2.54 ±0.68	2.11	1.77	27.66 ±5.23	2.19	1.82
B3	15.01 ±7.32	2.09	1.76	1.76 ±0.74	2.1	1.66	15.73 ±6.91	2.17	1.68
B4	36.01 ±9.11	2.19	1.76	2.8 ±0.23	2.16	1.76	32.41 ±10.11	2.17	1.76
C1	9.31 ±3.27	2.25	1.74	2.55 ±0.22	2.16	1.73	7.53 ±2.35	2.09	1.8
C2	20.06 ±11.8	2.24	1.82	3.35 ±0.51	2.13	1.78	23.6 ±9.21	2.22	1.8
C3	11.93 ±4.23	2.11	1.65	2.13 ±1.03	2.08	1.65	11.17 ±5.67	2.05	1.71
C4	28.69 ±16.2	2.15	1.82	1.91 ±0.89	2.16	1.79	31.73 ±13.9	2.29	1.82
Mean	20.47	2.16	1.75	2.32	2.11	1.71	20.47	2.18	1.75
S.D.	8.31	0.06	0.05	0.45	0.05	0.06	8.14	0.07	0.05

[a] See figure 1.

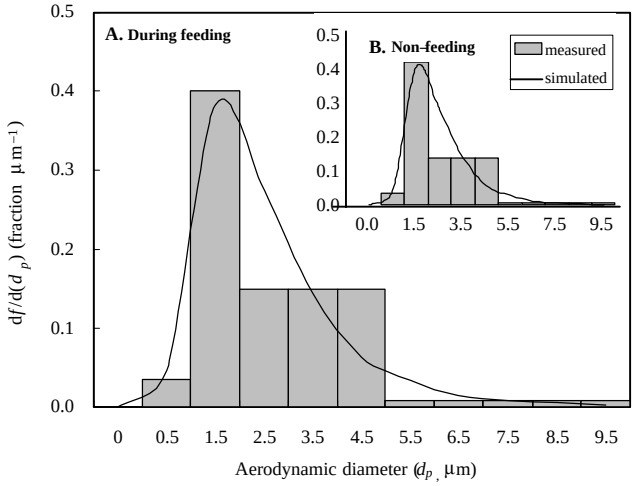

Figure 2. Lognormal size distribution model fitted to the experimental data for feeding and non–feeding periods.

appears to be extremely high. The high values might be related to the feeding strategy and feedstuff used in the Tainan swine building.

Two different lognormal aerosol size distributions were considered as the aerosol profiles in the model simulations: LN(2.17, 1.75) having 3980 particles cm^{-3} and LN(2.11, 1.71) having 455 particles cm^{-3} as observed in the Tainan swine building during feeding and non–feeding periods, respectively. An aerosol profile of LN(8, 3) as measured in a mechanically ventilated swine nursery by Maghirang et al. (1997) was calculated and also used in the model comparison.

Figure 3 shows the result of a simulation of the dust–borne toluene exposure as a function of time in a 24–h basis in the Tainan pig house. The contribution to the exposure dose and concentration from each size bin is shown. Figure 3A shows the dust–borne toluene concentrations rise while the feeding begins, peak at about the time the feeding is stopped, then fall with a decay rate dictated by the decrease in particle concentration since ventilation only partially removes the dust–borne toluene concentration from the previous feeding.

Figure 3B is a plot of the cumulative inhalation dose of dust–borne toluene as a function of time. The total integrated dose is also shown (fig. 3C). The inhalation dose continues to increase for a considerable period after the feeding is stopped. This feature makes the time spent of workers in the pig house after feeding an important parameter to be considered in dose reduction. Since the number of particles is relatively small for bins 1, 4, and 5 (table 3), the dominant contribution to the dose is from bins 2 and 3 (average particle sizes are 1.85 and 2.75 μm, respectively). Figure 3B also indicates that the integrated doses at the times the feeding is stopped at 07:00 and 19:00 are around 4×10^{-2} and 13.5×10^{-2} μg kg^{-1} for 1.85 and 2.75 μm aerosol and 2×10^{-2} and 6.5×10^{-2} μg kg^{-1} for 0.95 and 3.65 μm aerosol, respectively. Calculations using the model also indicate that the integrated dose for the *n*th feeding is roughly (2*n*–1) times the integrated dose for the first feeding.

Table 5 gives the simulation results of adsorption and deposition rates of dust–borne toluene in feeding and non–feeding periods. Table 5 indicates that the orders of magnitude of adsorption rate are 10^3 and 10^1 h^{-1}, respectively, for particle sizes in the range of 2 to 3 μm AED in feeding and non–feeding periods. This effect is shown in equation 4 in which adsorption rate and particle concentration are directly proportional. Because particle size distributions are time–dependent, the orders of magnitude of deposition rates are 10^{-3} and 10^{-5} h^{-1} in feeding and non–feeding periods, respectively.

Figure 4 shows the simulation performed for feeding and non–feeding periods. Specifically, figure 4 indicates that at the same initial condition the dust–borne toluene concentrations were reduced from 2.5×10^{-3} to 6.5×10^{-4} mg m^{-3} and the inhalation doses were reduced from 5.8×10^{-4} to 3.5×10^{-5} μg kg^{-1}, respectively, in feeding and non–feeding

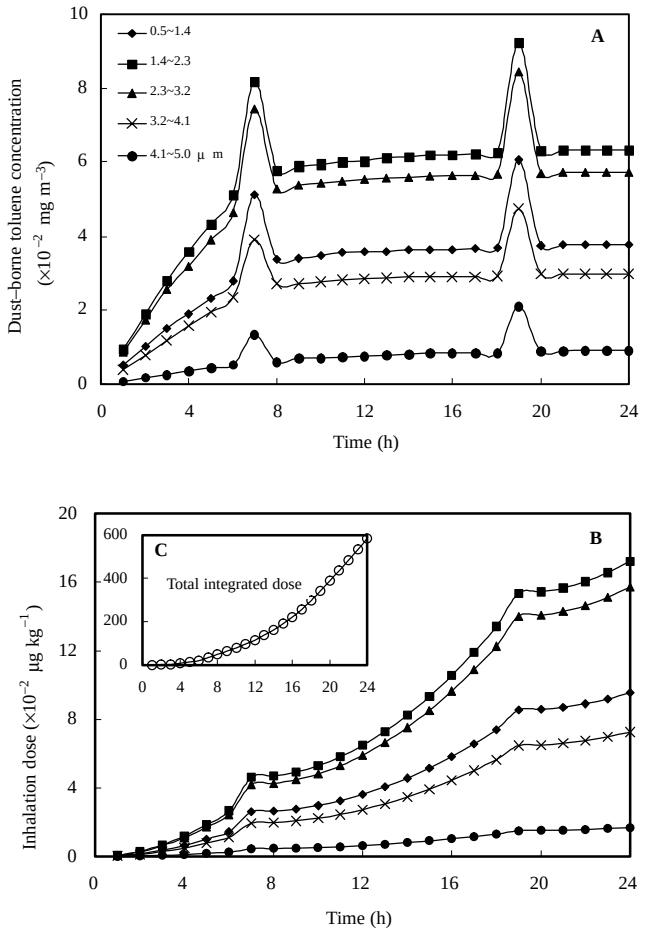

Figure 3. Simulation results of: (A) time evolution of dust–borne toluene concentration in a 24–h basis of each size bin of the Tainan pig house, (B) cumulative inhalation dose of dust–borne toluene as a function of time, and (C) the total integrated exposure dose.

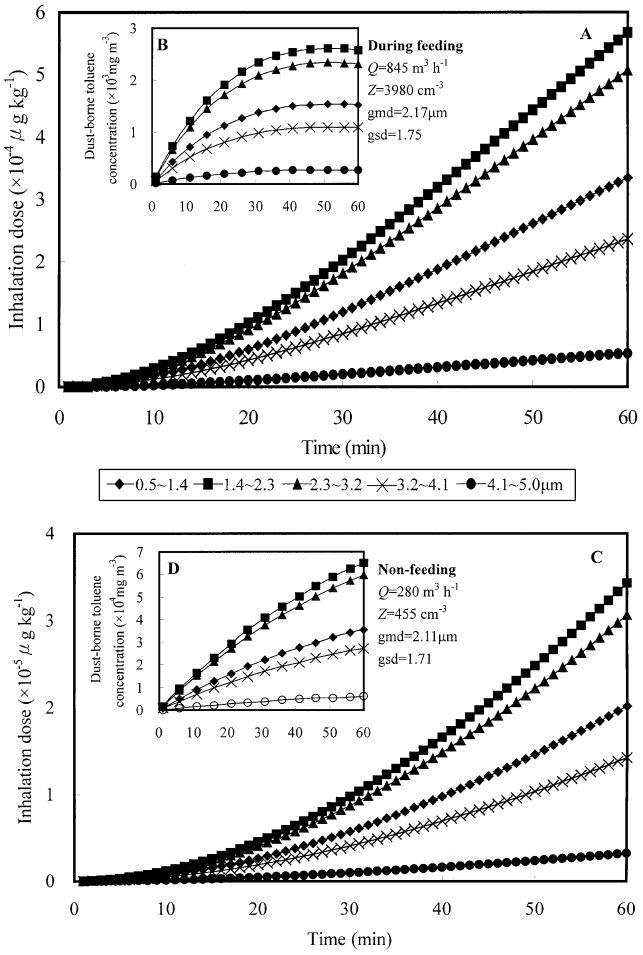

Figure 4. Time evolution of concentration and inhalation dose of dust–borne toluene from simulation of the Tainan pig house during (A and B) feeding and (C and D) non–feeding periods.

Table 5. A summary of simulation results of adsorption and deposition rates in feeding and non–feeding periods.

	Bin number (k)	Adsorption rate ($\lambda_a(k)$, h^{-1})	Deposition rate ($\lambda_d(k)$, h^{-1})
Feeding period			
	1 (0.5~1.4μm)	9.7×10^2	4.2×10^{-4}
λ_v = 1.9 h^{-1}	2 (1.4~2.3μm)	1.6×10^3	6.5×10^{-4}
Z = 3980 cm^{-3}	3 (2.3~3.2μm)	1.4×10^3	2.6×10^{-3}
GMD = 2.17μm	4 (3.2~4.1μm)	6.9×10^2	1.5×10^{-2}
GSD = 1.75	5 (4.1~5.0μm)	1.7×10^2	9.7×10^{-2}
Non–feeding period			
	1 (0.5~1.4μm)	1.1×10^2	4.1×10^{-4}
λ_v = 0.63 h^{-1}	2 (1.4~2.3μm)	1.9×10^2	6.1×10^{-4}
Z = 455 cm^{-3}	3 (2.3~3.2μm)	1.7×10^2	2.1×10^{-3}
GMD = 2.11μm	4 (3.2~4.1μm)	7.9×10^1	1.1×10^{-3}
GSD = 1.71	5 (4.1~5.0μm)	1.9×10^1	6.5×10^{-2}

periods for 1.85 μm aerosol. Figures 4A and 4C show that the equilibrium occurs earlier as the ventilation rate increases.

Figure 5 shows the results of simulation performed for the two aerosol profiles (LN(2.17, 1.75) and LN(8, 3)) by varying the feeding duration and the time spent in the pig house after feeding period for workers. The breathing rate of 15 m^3 d^{-1} (10 L min^{-1}) for a 70 kg worker was used in the simulation. Each symbol corresponds to a fixed duration of feeding. Even though the exposure dose is initially nonlinear as a function of time, a few minutes after the feeding period is ended it is linear to a good approximation. Hence, the doses are approximately linear with respect to the time spent in the pig house after the feeding period.

The exposure dose continues to rise after the feeding period is ended (fig. 3). As a result, the dose for a short feeding duration followed by a long stay in the pig house can equal that of a long feeding duration followed by a short subsequent exposure. Reduction of both the feeding duration and/or subsequent time in the pig house is highly effective in dose reduction. Figure 5 shows that for the small diameter aerosol (GMD = 2.17 μm) the equivalent dose for a 3 h feeding duration followed by 3 h in the pig house is about 3×10^{-3} μg kg^{-1}, while that for a 2 h feeding duration followed by 2 h in the pig house is about 1.5×10^{-3} μg kg^{-1}. For the large diameter aerosol (GMD = 8 μm), the corresponding reduction is from 8.5×10^{-4} to 4×10^{-4} μg kg^{-1}.

In order to get insight into the effect of existing aerosol profile, the simulations were performed for two different aerosol profiles (LN(2.17, 1.75) and LN(8, 3)) at the feeding and non–feeding operating conditions. Also shown in figures 6C, D and 7C, D are the snapshots of the dust–borne toluene size distribution corresponding to the concentration profiles of figures 6A, B and 7A, B at 5, 10, 20, 40, and 60 min. Figures 6 and 7 reveal several implications: (1) the particle

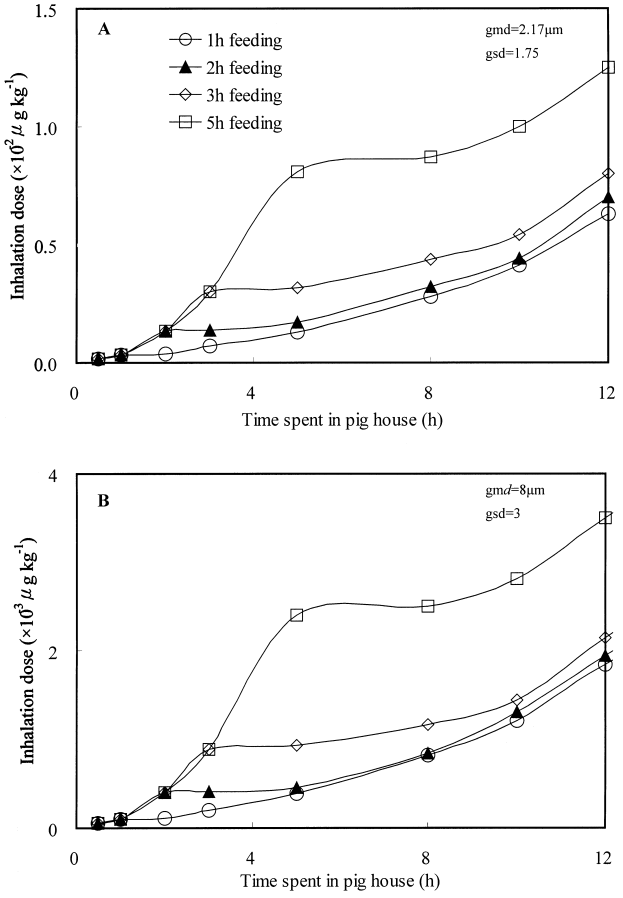

Figure 5. Simulation results for two aerosols of (A) 2.17 μm GMD and (B) 8 μm GMD by varying the feeding duration and the time spent in the pig house for one worker. The air exchange rate is 1.9 h^{-1} and the particle concentration is 4000 cm^{-3} for both cases.

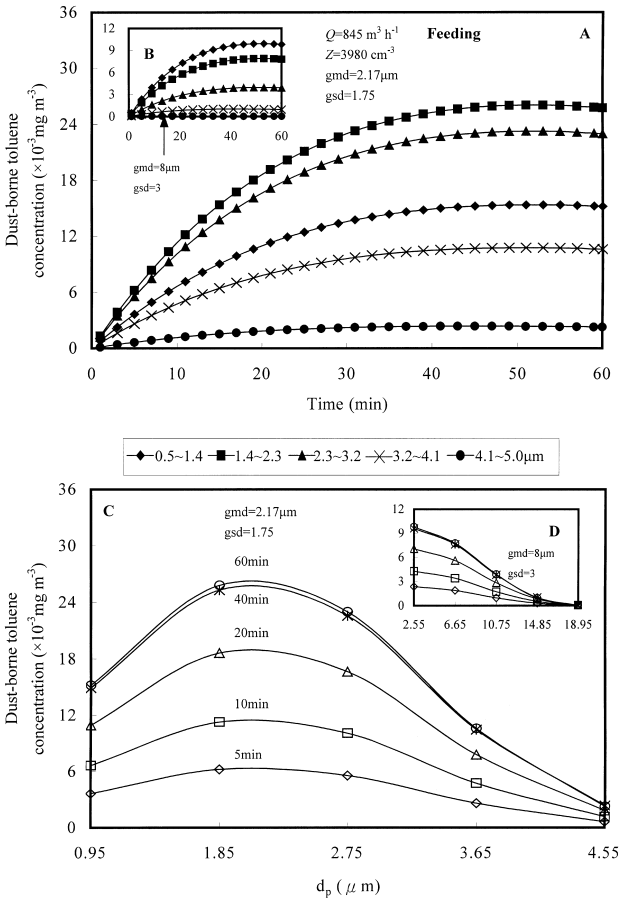

Figure 6. Simulation results performed for two aerosol of 2.17 μm GMD and 8 μm GMD during feeding period of (A) time evolution of dust–borne toluene concentration and (B) dust–borne toluene size distribution corresponding to the above concentration profiles at 5, 10, 20, 40, and 60 min.

diameter ranging from 1.5 to 2.75 μm lead to greater adsorption, which keeps the dust–borne toluene airborne, whereas the larger particles of >3.65 μm are more effectively removed by deposition; thus, changes in particle size to a larger size could lower maximum dust–borne VOC–odor concentrations; (2) the changes in sizes will affect the deposition of particles onto the enclosure surfaces and thus affect the amount of dust–borne VOC–odor available for inhalation; and (3) the changes in size will alter where the particles deposit within the respiratory tract; if the number of particles is relatively small, adsorption is low and the dominant contribution to the exposure dose for workers and animals is from the fine dust–borne VOC–odor.

The consideration of size distribution therefore is important in exposure dose assessment due to its sensitivity on the size of the inhaled particle carrying VOC–odor. Airborne dust may undergo some hygroscopic growth in the high humidity environment in the pig houses, e.g., in a misting system. If the fine airborne dust between 0.5 to 1 μm can grow to large sizes between 1.5 to 2.75 μm, then this increase will result in a large adsorption rate of VOC–odor to the existing aerosol. Also if the aerosol can grow in the high humidity achieved during misting, then it can grow in the respiratory tract. Therefore, when the dust–borne VOC–odor entering the lung is reduced, the amount of possible growth depends on how close the relative humidity in pig houses is to 100% and further alters the deposition patterns within the lung.

Simulations were also performed for three different pig house sizes measured in surface to volume ratios (*S*/*V*) of 0.3, 0.5, and 1 m^{-1} (fig. 8). Figure 8 indicates that the changes in dust–borne toluene exposure dose due to the changes in surface to volume ratio varied significantly. It was found that, to a very good level of approximation, the inhalation dose varies directly as the volume of the pig house. This is to be expected since the dust–borne VOC–odor concentration is directly proportional to the pig house volume. From a theoretical point of view, as the pig house volume increases, its surface to volume ratio decreases, and this leads to a lower rate of surface deposition of dust–borne VOC–odor.

However, there is an additional factor. As the pig house volume increases, the air exchange rate decreases or the residence time of airflow rate increases at the same ventilation rate, and this leads to a higher dust–borne VOC–odor concentrations. Figure 8 also shows that as the surface to volume ratio increases, the time to reach the maximum dose decreases, and the maximum dose decreases. Therefore, increased surface to volume ratio not only lowers maximum dust–borne VOC–odor inhalation dose but it also causes the maximum dose to be reached in a shorter time.

Adsorption is a surface phenomenon, and not just a surface area phenomenon. On the derivation of Freundlich adsorption model, except surface area, surface tension and surface free energy of airborne dust are the key parameters in the adsorption equations (Weber and DiGiano, 1996). The final

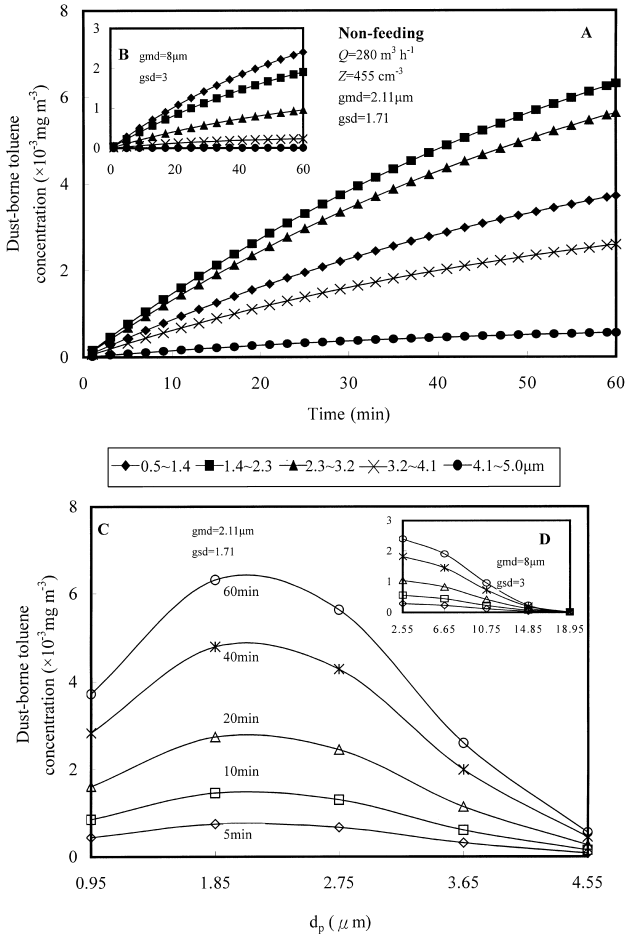

Figure 7. Simulation results performed for two aerosol of 2.17 μm GMD and 8 μm GMD during non–feeding period of (A) time evolution of dust–borne toluene concentration and (B) dust–borne toluene size distribution corresponding to the above concentration profiles at 5, 10, 20, 40, and 60 min.

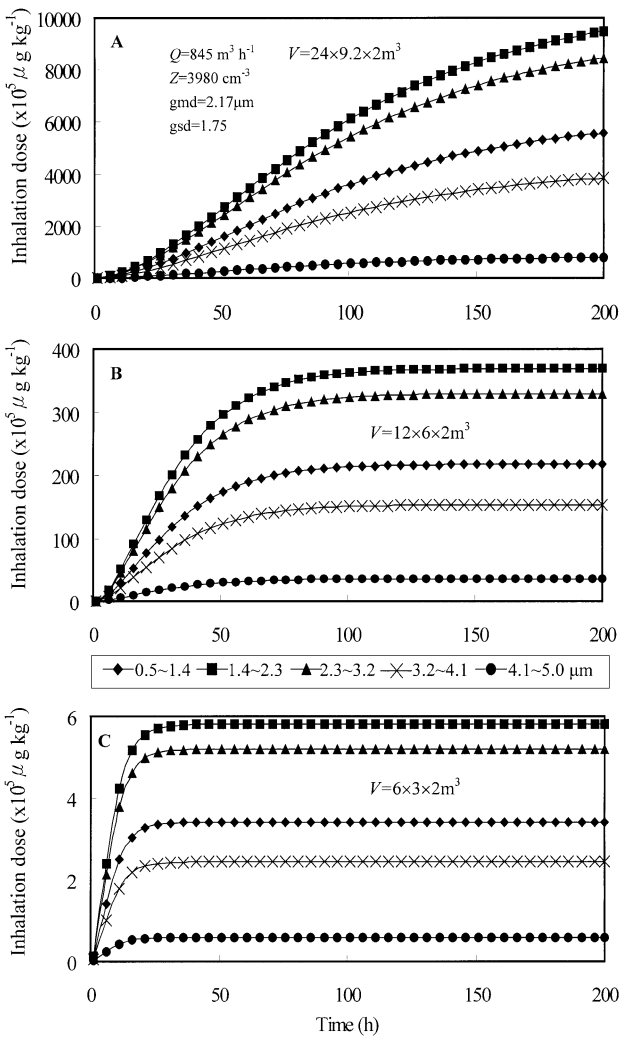

Figure 8. Simulation results performed by varying surface to volume ratios of pig house (*S*/*V*) of (A) 0.3, (B) 0.5, and (C) 1 m^{-1} for time evolution of dust–borne toluene inhalation dose.

expression for characteristics of the adsorption reaction is reflected by the adsorption capacity constant (K_F) and the adsorption intensity constant (n_F) in Freundlich adsorption model: $q_e = K_F C_{v,e}^{n_F}$ where q_e is the amount adsorbed in equilibrium with bulk VOC–odor concentration (kg kg^{-1}). AED is defined in terms of their aerodynamic behavior rather than their geometric properties. In many situations, it is not necessary to know the true size, shape factor, and density of a particle if its AED is known (Hinds, 1999). Therefore, AED is a suitable surrogate for actual particle diameter used in the adsorption processes between VOC–odor and existing airborne dust.

SUMMARY AND CONCLUSIONS

A dynamic, size–dependent integrated inhalation dose model for quantifying worker/animal exposure to dust–borne odor causing volatile organic compound (VOC–odor) in swine building during and after the time of feeding was developed. The inhalation dose model was then applied to a growing pig barn to assess the dust–borne VOC–odor exposure. The following results were obtained:

1. The exposure of dust–borne VOC–odor observed in pig barns can be characterized by adsorption and deposition of airborne dust. The airborne dust particle size, aerosol profile, enclosure dimension, ventilation rate, and feeding duration were affecting the integrated inhalation model in evaluating dust–borne VOC–odor exposure during and after the time of feeding.
2. There is no significant variation in feeding and non–feeding periods for particle size distributions and both followed a lognormal distribution with geometric mass mean diameter of 2.14 ±0.03 μm AED and geometric standard deviation of 1.73 ±0.02 in a growing pig barn located in the southern region of Taiwan. This work also indicates that feed dust was the main source of the existing airborne dust.
3. The smaller particle keeps the dust–borne VOC–odor airborne, whereas the larger particles are more effectively removed by surface deposition, and hence, an increase of the size of airborne dust can reduce the dust–borne VOC–odor inhalation dose. The inhalation dose for a short feeding duration followed by a long stay in the pig barn can equal that of a long feeding duration followed by a short subsequent exposure. Reduction of both the feeding duration and/or subsequent time in the pig barn is highly effective in dose reduction.

4. The model analysis shows that there can be a large variability in the dose depending on the exposure conditions. Since dynamic measurements are not usually available for the size distribution of the VOC–odor concentration, the model provides a conceptual framework for theoretical analysis to extrapolate beyond the immediate experimental results.

ACKNOWLEDGEMENTS

The authors appreciate the contributive comments by the anonymous referees. The authors wish to acknowledge the financial support of the National Science Council of Republic of China under Grant NSC 89–2621–B–002–043.

REFERENCES

Barth, C. L., L. F. Elliot, and S. W. Melvin. 1982. Using odor control technology to support animal agricultural. ASAE Paper No. 82–4035. St. Joseph, Mich.: ASAE.

Corner, J., and E. D. Pendlebury. 1951. The coagulation and deposition of stirred aerosol. *Proc. Phys. Soc.* B46: 645–654.

Crump, J. G., and J. H. Seinfeld. 1981. Turbulent deposition and gravitational sedimentation of an aerosol in a vessel of arbitrary shape. *J. Aerosol Sci.* 12(5): 405–415.

DeJours, P. 1968. *Respiration.* New York, N.Y.: Oxford University Press.

Gao, W., and J. J. R. Feddes. 1993. Using swine dust to verify a lumped–parameter model in a ventilated enclosure. *Canadian Agric. Eng.* 35(1): 67–73.

Geankoplis, C. J. 1993. *Transport Processes and Unit Operations*. 3rd ed. Englewood Cliffs, N.J.: Prentice–Hall.

Hammond, E. G., P. Kuczala, G. A. Junk, and J. Kozel. 1974. Constituents of swine house odors. In *Proc. International* Symposium on Livestock Environment, 364–372. St. Joseph, Mich.: ASAE.

Hammond, E. G., C. Fedler, and G. Junk. 1979. Identification of dust–borne odors in swine confinement facilities. *Trans. ASAE* 22(5): 1186–1189.

Hangartner, M. 1990. Selection and treatment of panelists for determination of odor thresholds. In *Odor Prevention* and Control of Organic Sludge and Livestock Farming, 55–60. V. C. Nielsen, J. H. Vooburg, and P. l'Hermite, eds. New York, N.Y.: Elsevier.

Hinds, W. C. 1999. *Aerosol Technology: Properties, Behavior, and Measurement of Airborne Particles*. 2nd ed. New York, N.Y.: John Wiley.

Howard, P. H., R. S. Boethling, W. F. Jarvis, W. M. Meylan, and E. M. Michalenko. 1991. *Handbook of* Environmental Degradation Rates. Chelsea, Mich.: Lewis Pub. Inc.

Jury, W. A., D. Russo, G. Streile, and H. E. Abd. 1990. Evaluation of volatilization by organic chemicals residing below the soil surface. *Water Resources Research* 26(1): 13–20.

IMSL MATH/LIBRARY. 1994. *FORTRAN Subroutine for Mathematical Applications*, Vol. 1. Houston, Tex.: Visual Numerics, Inc.

Liao, C. M., and J. J. R. Feddes. 1991. Modeling and analysis of airborne dust removal from a ventilated airspace. *Canadian Agric. Eng.* 33(2): 355–361.

_____. 1992. A lumped–parameter model for predicting airborne dust concentration in a ventilated airspace. *Trans. ASAE* 35(6): 1973–1978.

Liao, C. M., and S. Singh. 1998. Modeling dust–borne odor dynamics in swine housing based on age and size distributions of airborne dust. *Applied Math. Modeling* 22(9): 671–685.

Liao, C. M., and H. M. Liang. 2000. Modeling effects of moisture content and advection on odor causing VOCs volatilization from stored swine manure. *J. Environ. Sci. Health* B35(3): 357–378.

Liu, Y. 1997. Methods for measuring fan ventilation rates in livestock buildings. Unpublished MS thesis. Manhattan, Kansas, Kansas State University.

Maghirang, R. G., M. C. Puma, Y. Liu, and P. Clark. 1997. Dust concentrations and particle size distribution in an enclosed swine nursery. *Trans. ASAE* 40(3): 749–754.

Miner, J. R. 1982. Controlling odors from livestock production facilities. In *Research Results in Manure Digestion,* Runoff, Refeeding*, and Odor,* 30–35. North Central Regional Research, Pub. No. 284. Ames, Iowa: Midwest Plan Service, Iowa State University.

Mount, L. E. T. 1968. *The Climatic Physiology of the Pig*. London, U.K.: Edward Arnold.

Nazaroff, W. W., and G R. Cass. 1989. Mass–transport aspects of pollutant removal at indoor surfaces. *Environ. Int.* 15: 567–584.

Nazaroff, W. W., M. P. Ligocki, T. Ma, and G. R. Cass. 1990. Particle deposition in museums: Comparison of modeling and measurement results. *Aerosol Sci. Tech.* 13(3): 332–348.

Perkins, S. L., and J. J. R. Feddes. 1996. The effects of timing of floor–application of mineral oil on dust concentrations in a swine farrowing unit. *Canadian Agric. Eng.* 38(2): 123–127.

Thibodeaux, L. J. 1996. *Environmental Chemodynamics*. 2nd ed. New York, N.Y.: John Wiley.

Van Loy, M. D., V. C. Lee, L. A. Gundel, J. M. Daisey, R. G. Sextro, and W. W. Nazaroff. 1997. Dynamic behavior of semivolatile organic compounds in indoor air. 1. Nicotine in a stainless steel chamber. *Environ. Sci. Tech.* 31(9): 2554–2561.

Van Wicklen, G. L., and M. F. Yoder. 1988. Respirable aerosol concentrations in an enclosed swine nursery. *Trans. ASAE* 31(6): 1798–1803.

Weber, Jr. W. J., and F. A. DiGiano. 1996. *Process Dynamics and Environmental Systems*. New York, N.Y.: John Wiley.

Yasuhara, A. 1980. Relation between odor and odorous components in swine manure. *Chemosp*here 9: 587–592.

Yasuhara, A., and K. Fuwa. 1979a. Volatile and odorous components in solid swine manure. *Agric. Biol. Chem.* 43(2): 313–316.

_____. 1979b. Quantification of phenols in gas from rotten liquid swine manure by computer–controlled gas chromatography–mass spectrometry. *Bull. Chem. Soc. Japan* 52(11): 3311–3313.

_____. 1979c. Odor and volatile compounds in liquid swine manure: Volatile and odorous components in anaerobically or aerobically digested liquid swine manure. *Bull. Chem. Soc. Japan* 52(1): 114–117.

Yasuhara, A., K. Fuwa, and M. Jimbu. 1983. Isolation and analysis of odorous compounds in swine manure. *J.* Chromatogr. 281: 225–236.

_____. 1984. Identification of odorous compounds in fresh and rotten swine manure. *Agric. Biol. Chem.* 48(12): 3000–3010.

Zhang, Y., A. Tanaka, E. M. Barber, and J. J. R. Feddes. 1996. Effects of frequency and quantity of sprinkling canola oil on dust reduction in swine buildings. *Trans. ASAE* 39(3): 1077–1081.

APPENDIX: NOMENCLATURE

A	Manure pit area, m^2
$B_r(t)$	Breathing rate of the worker or animal at time t, L min^{-1}
B_w	Body weight of the worker or animal, kg
C(k,t)	Time–dependent dust–borne VOC–odor con–centration in the *k*th size range, kg m^{-3}
C_s	Initial VOC–odor concentration in slurry column, g m^{-3}
C_{slip}	Slip correlation factor, dimensionless
$C_v(t)$	Time–dependent VOC–odor concentration,

	kg m^{-3}
$C_{v,e}$	Steady–state VOC–odor concentration, kg m^{-3}
d_g	Geometric mean diameter (GMD), μm
d_{max}	the largest particle size, μm
d_{min}	the finest particle size, μm
d_p	Particle diameter, μm
$D(d_p)$	Brownian diffusion coefficient of a particle of diameter d_p, m^2 s^{-1}
D(k,t)	Time–dependent cumulative exposure dose per unit body weight of worker or animal in the *k*th size bin, μg kg^{-1}
D_E	Effective diffusion coefficient of VOC–odor in the slurry, m^2 s^{-1}
D_g^a	Diffusion coefficient of VOC–odor in air, m^2 s^{-1}
D_l^w	Diffusion coefficient of VOC–odor in water, m^2 s^{-1}
D_s	Surface effective diffusivity of VOC–odor in the air, m^2 s^{-1}
$f(d_p)$	Particle size distribution function, dimensionless
f_{oc}	Fraction of roganic carbon, dimensionless
g	Gravitational acceleration constant, m s^{-2}
H_E	Horizontal moisture velocity, cm d^{-1}
$J_s(0,t;W)$	Time–dependent VOC–odor flux from manure pit, g m^{-2} s^{-1}
K_F	Freundlich capacity constant, m^3 kg^{-1}
K_H	Henry's law constant, dimensionless
K_{oc}	Organic carbon distribution coefficient, m^3 kg^{-1}
k	Size range number
k_B	Boltzmann's constant, erg $°K^{-1}$
k_e	Turbulent intensity parameter, dimensionless
l, w, h	Length, width, and height of the enclosure, m
LN	Lognormal probability density function
N	End point number for a *k*th size range between d_k and d_{k+1}.
n	Exponent in deposition rate equation, dimensionless
n_F	Freundlich intensity constant, dimensionless
Q	Ventilation rate, m^3s^{-1}
q_e	amount adsorbed in equilibrium with bulk VOC–odor concentration, kg kg^{-1}
S	Surface area of enclosure, m^2
S(t)	VOC–odor source strength, g s^{-1}
T	Indoor absolute temperature, °K
V	Volume of enclosure, m^3
V_E	Vertical moisture velocity, cm d^{-1}
$v_s(d_p)$	Settling velocity of a particle of diameter d_p, m s^{-1}
W	Contaminated layer thickness of slurry, m
Z	Particle concentration, cm^{-3}
$\beta(d_p)$	Adsorption coefficient of VOC–odor to the surface of an airborne dust with diameter d_p, m^3 h^{-1}
$\gamma(k)$	Fraction of the VOC–odor taken into the total lung volume that is available for uptake for *k*th size bin, dimensionless
η_a	Dynamic viscosity of air, p
λ	Mean free path of air, cm
$\lambda_a(d_p)$	Adsorption rate of VOC–odor to aerosol surface in the of particle diameter d_p, h^{-1}
$\lambda_a(k)$	Adsorption rate of VOC–odor to aerosol surface in the *k*th size range, h^{-1}
$\lambda_d(d_p)$	Deposition rate of dust–borne VOC–odor of particle diameter d_p, h^{-1}
$\lambda_d(k)$	Deposition rate of dust–borne VOC–odor in the *k*th size range, h^{-1}
λ_i	First–order decay rate constant of VOC–odor, h^{-1}
λ_v	Air exchange rate, h^{-1}
ρ_a	Density of the air, g cm^{-3}
ρ_p	Density of dust particle, kg m^{-3}
σ_g	Geometric standard deviation (GSD), dimensionless
$\Phi(d_p)$	Size–dependent diffusion length modulus, dimensionless
$\bar{\tau}$	Nominal residence time of ventilation air, h